Assessment of the Absorbed Dose Variations in the Thyroid Gland Exposed to Orthopantomography (OPG) while Swallowing: A Novel Approach to Radiation Protection

Hassan Vafapour (PhD Candidate)[1], Zaker Salehi (PhD)[1]*

[1]Department of Radiation Sciences, School of Paramedical Sciences, Yasuj University of Medical Sciences, Yasuj, Iran

ABSTRACT

Background: The reliance on specialized diagnostic techniques is on the rise across various medical fields, including dentistry. While orthopantomogram (OPG), offers many advantages in terms of dental diagnosis, it also poses potential risks to sensitive organs, notably the thyroid gland.

Objective: This study aimed to evaluate the fluctuations in the absorbed dose within the thyroid gland during swallowing while undergoing an OPG procedure.

Material and Methods: In this computational simulation study, the BEAMnrc Monte Carlo code was employed to model an OPG machine, using 700 million particles across the energy range of 60-75 keV, which is standard for OPG procedures. The Monte Carlo (MC) model was cross-verified by comparing the derived spectra with those in the IPEM Report 78. A head and neck phantom was constructed using CT scan images with a slice thickness of 5 mm. This phantom underwent simulated beam exposure under two conditions: pre-swallow and post-swallow. Subsequently, the percentage depth dose was measured and contrasted across different depths.

Results: After swallowing, there was an increase in the absorbed dose across all three regions of the thyroid (right, left, and center). Notably, regions near the hyoid bone exhibited a particularly significant increase in dose. In certain areas, the absorbed dose even tripled when compared to the pre-swallowing state.

Conclusion: The findings indicate that during OPG imaging, swallowing can lead to an increased radiation dose to the thyroid gland. Given the thyroid's heightened sensitivity to radiation, such an increase in dosage is noteworthy.

Citation: Vafapour H, Salehi Z. Assessment of the Absorbed Dose Variations in the Thyroid Gland Exposed to Orthopantomography (OPG) while Swallowing: A Novel Approach to Radiation Protection. *J Biomed Phys Eng*. 2024;14(3):267-274. doi: 10.31661/jbpe.v0i0.2305-1622.

Keywords

Monte Carlo Method; Thyroid Gland; Radiography; Panoramic

Introduction

Recently, dental professionals have increasingly prescribed oral and dental radiographs to enhance the diagnostic accuracy of patients' dental conditions. Among these radiographs, Orthopantomogram (OPG), also known as dental panoramic imaging, stands out as one of the most essential and commonly employed techniques [1]. In this radiographic equipment, a single frame displays a two-dimensional representation of both the upper and lower jaw teeth [2]. Through OPG

*Corresponding author:
Zaker Salehi
Department of Radiation Sciences, School of Paramedical Sciences, Yasuj University of Medical Sciences, Yasuj, Iran
E-mail:
Phyzaker@gmail.com

Received: 20 May 2023
Accepted: 11 September 2023

imaging, dentists can effortlessly evaluate the condition of a patient's teeth, from the crown to the root. Additionally, they can anticipate the health of the patient's unaffected teeth. This ease and comprehensive insight have resulted in a surge in requests for this imaging technique. Consequently, in many clinics, dental treatments involving restorative procedures often commence with an OPG [2]. Considering that the OPG radiation exposure lasts about 15 seconds, it is notably longer than many other two-dimensional radiographic imaging techniques [3, 4]. It's worth mentioning that while the National Radiological Protection Board (NRPB) suggests a reference value of 65 mGy per year for dental panoramic radiography, the ALARA (As Low As Reasonably Achievable) principle is also emphasized. This is especially pertinent given the heightened sensitivity of tissues exposed to radiation, particularly the thyroid. [3-5]. The thyroid gland is the largest gland in the neck [6,7]. The thyroid is a butterfly-shaped gland situated in the neck, consisting of two lobes located on either side of the windpipe. This gland measures approximately 2 inches (5 cm) across and sits just beneath the Adam's apple [8]. This gland is strategically positioned in the neck, with a portion situated anteriorly and the remaining extending to either side of the trachea. Given its location, during OPG procedures, it's conceivable that the entire thyroid or parts of it will be subjected to radiation exposure. Due to the gland's sensitivity, such exposure can pose potential risks, emphasizing the importance of protective measures to minimize radiation-induced harm. Although thyroid shields are designed to reduce radiation exposure, they can sometimes produce artifacts that compromise the image quality. As a result, to ensure clear imaging, thyroid shields are either not used or are positioned away from the lower jaw in many instances. The narrow imaging field of OPG allows for a significant portion of the thyroid to be excluded from the radiation field. However, upward movement of the thyroid could bring it entirely within the radiation field. It's been documented that during swallowing, the thyroid, in conjunction with the trachea, can ascend between 1.5 to 3.5 cm, thereby increasing its exposure riskGiven that an individual typically swallows between 500 to 700 times daily, averaging about once per minute, there's a notable likelihood of swallowing occurring during the duration of OPG irradiation, especially given its extended exposure time. This raises concerns about the potential increased risk of thyroid exposure during the imaging process [9]. The primary aim of this study was to evaluate the changes in the absorbed radiation dose to the thyroid when it moves into the Field of View (FOV) due to swallowing during an OPG procedure.

Material and Methods

In this computational simulation study, we utilized the BEAMnrc Monte Carlo code, processing over 700 million particles. The study focused on a Planmeca ProMax machine equipped with a 2.5 mm aluminum filter, operating within the standard OPG energy range of 60-75 keV.CT images of a patient's neck, sourced from the hospital's database and having a slice thickness of 5 mm, were utilized to create a digital phantom, which was employed as the thyroid phantom for our study. The required density and Hounsfield numbers (HU) for the phantom simulation were obtained from a Monte Carlo model developed by Zhou et al., [10]. To validate the simulation model, The X-ray spectrum obtained from the current study was directly compared with the radiation spectrum derived from IPEM Report 78 [11]. Monte Carlo simulations were executed for two scenarios: pre-swallow and post-swallow. The images on the left and right of Figure 1 represent the conditions before and after swallowing, respectively. Simulations were developed for three points located in the thyroid (left, right, and center) and Depth-Dose graphs were obtained at different depths of the thyroid phantom.

Results

Figure 2 shows the X-ray spectrum obtained from the Monte Carlo (MC) model of the current study for 70 keV compared to IPEM Report 78.

Figure 2 illustrates that our the MC model aligns closely with the findings presented in IPEM Report 78 [11]. It's worth mentioning that the subtle variance between the spectra arises from the differences in anode angles. This study utilized an angle of 5 degrees, while the IPEM indicates that the smallest angle that can be employed is 6 degrees. Spectra for other energies (60, 65, and 75 keV) were derived using the same methodology as that of 70 keV. Figure 3 illustrates the ratio of Dose to maximum dose (D/D_{max}) for three distinct locations within the thyroid phantom: left, center, and right, both before and after swallowing. Concurrently, Table 1 presents the D/D_{max} values across all energy levels (60-75 keV) for these three specific locations. The left

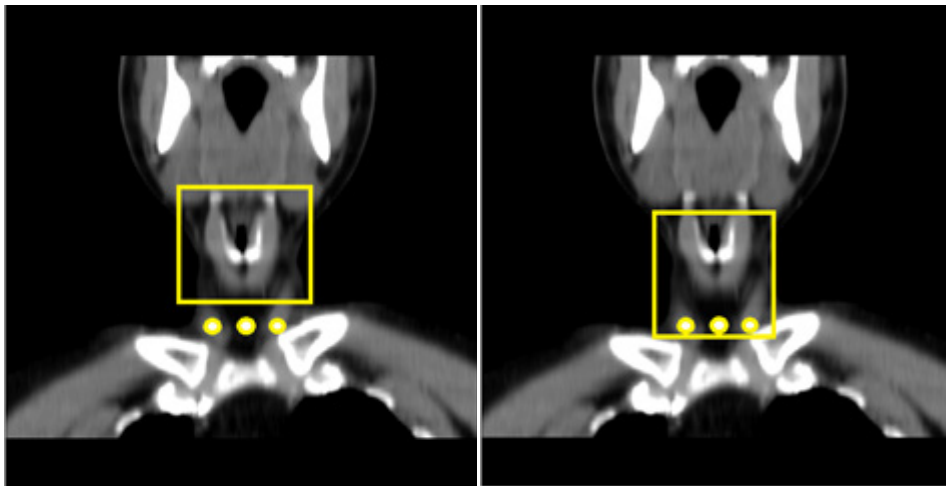

Figure 1: Left and right images represent before and after swallowing statuses respectively. Simulations were developed for three points located in the thyroid (left, right, and center) for both statuses.

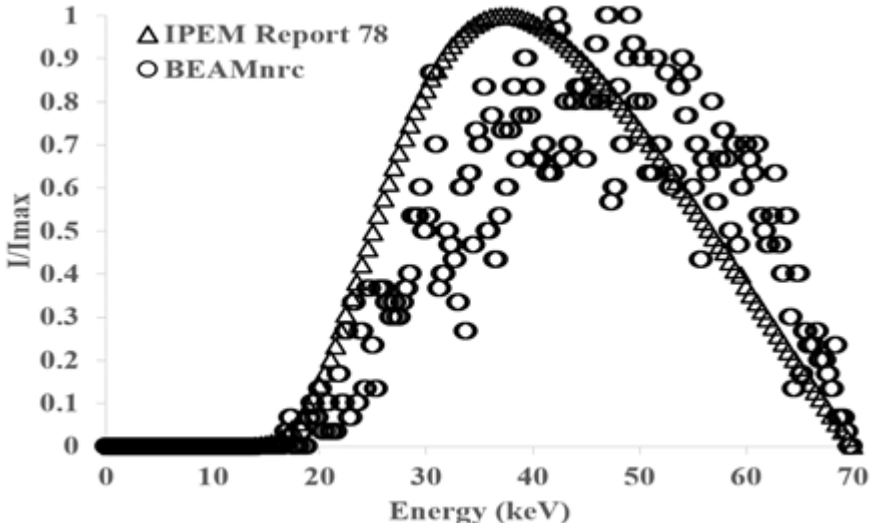

Figure 2: X-ray spectrum obtained from the Monte Carlo (MC) model of the current study and IPEM Report 78.

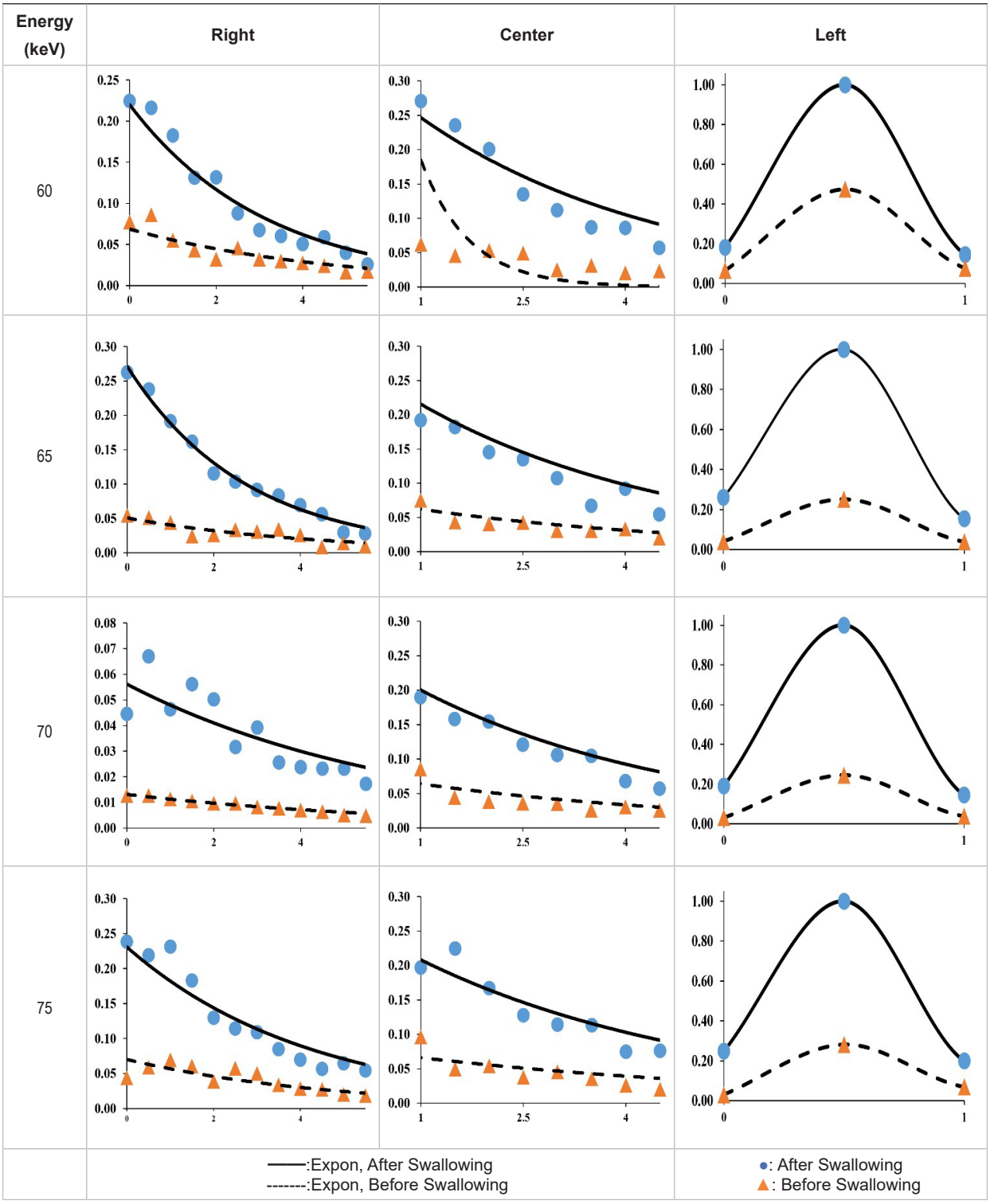

Figure 3: D/D_{max} versus Depth for all energies (60-75 keV) for three locations included (Left, center, and right). Each graph depicts two statuses included before and after swallowing. D_{max} for the graphs is calculated based on the maximum dose values for that energy (Expon: Exponential).

Table 1: $D/D_{total\text{-}max}$ versus Depth for all energies (60-75 keV) for three locations included (Left, center, and right). $D_{total\text{-}max}$ is calculated based on the maximum dose values among all energies.

Energy (keV)	Depth (cm)	Right			Center			Left		
		Before	After	Increase (%)	Before	After	Increase (%)	Before	After	Increase (%)
60	0	0.042	0.123	192.86	0.024	0.178	641.67	0.036	0.100	177.78
	2	0.018	0.072	300.00	0.029	0.110	279.31	0.017	0.060	252.94
	4	0.015	0.028	86.67	0.011	0.047	327.27	0.012	0.043	258.33
	6	0.043	0.079	83.72	0.014	0.060	328.57	0.010	0.010	0.00
65	0	0.043	0.207	381.40	0.083	0.281	238.55	0.032	0.206	543.75
	2	0.020	0.091	355.00	0.032	0.115	259.38	0.021	0.090	328.57
	4	0.020	0.055	175.00	0.026	0.073	180.77	0.014	0.049	250.00
	6	0.045	0.086	91.11	0.021	0.083	295.24	0.009	0.015	66.67
70	0	0.013	0.044	238.46	0.100	0.245	145.00	0.031	0.189	509.68
	2	0.01	0.05	400.00	0.038	0.154	305.26	0.045	0.114	153.33
	4	0.007	0.024	242.86	0.030	0.068	126.67	0.024	0.068	183.33
	6	0.011	0.063	472.73	0.034	0.085	150.00	0.025	0.032	28.00
75	0	0.044	0.238	440.91	0.063	0.232	268.25	0.030	0.247	723.33
	2	0.038	0.130	242.11	0.054	0.167	209.26	0.037	0.148	300.00
	4	0.029	0.070	141.38	0.026	0.075	188.46	0.024	0.083	245.83
	6	0.058	0.209	260.34	0.042	0.095	126.19	0.020	0.030	50.00

region of the thyroid exhibited a marked rise in absorbed dose, which can be attributed to the heightened probability of the photoelectric effect occurring in areas with greater density.

Discussion

The current research utilized MC codes (BEAMnrc) to quantify the alterations in dose impacting the thyroid gland during a 15-second jaw imaging (OPG) concurrent with oral fluid ingestion. For validation, X-ray spectra derived from these MC simulations were juxtaposed with data from IPEM 78, taking into account the filter parameters as specified by the manufacturer. The X-ray spectrum obtained by the BEAMnrc simulation has been standardized to the IPEM spectrum at the maximum number of photons independent of the characteristic K-edge X-rays [11]. The results showed that the X-ray spectra in the energy range match well, but the level of this accord was less in the lower energies. This dissimilarity can be attributed to the tiny difference in anode angle in the simulator and IPEM. On the other hand, the energy range of OPG device rays is between 60 and 75 kVp [11]. Due to 1.7 to 3.5 cm displacement of the thyroid during adult swallowing relative to before, this difference was set to be 3 cm in this study (Figure 1) [9].

This study evaluated the change in absorbed dose due to the 3 cm displacement of the thyroid. During OPG imaging, primary and scatter radiation produce doses to sensitive tissues such as the thyroid. Unlike primary radiation, scatter radiation is mainly generated from the patient body and bed. In OPG, however, the beam field is very narrow and radiation is restricted to the face, particularly in the mandible. In addition to narrowing the field size, thyroid shields are also used to prevent direct radiation in radiation centers. However, due to the image artifacts caused by lead, most of the OPG operators prefer to either not use the

shield or to use it at a distance from the lower jaw. On the other hand, according to the thyromental distance (TMD), which is about 6 and a half centimeters, it can be concluded that at least a part of the thyroid will be placed in the primary radiation field during imaging. Moreover, swallowing during OPG imaging can reduce the distance between the thyroid and mandible to almost half, and therefore most of the thyroid will be placed in the field of the primary rays (Figure 1).

Figure 3 depicts the normalized lateral and depth dose profiles before and after swallowing across various energy levels (60, 65, 70, and 75 keV) utilized by the OPG machine. The profile of the dose depth in the central and lateral parts of the thyroid exhibited a significant disparity between the pre- and post-swallowing doses across all energy levels. The difference was more pronounced in the lateral regions of the thyroid compared to the central part. Notably, the presence of the clavicle on the left side introduced variations in the dose profile, distinct from the right and central points. The photoelectric effect caused an increase in dose at a specific depth due to the influence of the clavicle. To mitigate this effect, it is advisable to position the patient's shoulders in a downward tilt during the procedure. This adjustment serves two purposes: reducing artifacts caused by the shoulder girdle bones (such as the clavicle, humerus head, and scapula) and minimizing scattered radiation that can elevate the dose in sensitive organs like the thyroid. Additionally, the presence of hyoid bones and cervical vertebrae contributes to backscattered radiation, potentially leading to an increased dose in the thyroid. Studies have shown that bone and metal objects can result in an approximate 10% increase in absorbed dose in the skin and soft tissues. This effect is particularly important to consider in radiation-sensitive areas like the thyroid [13-15].

The data presented in Table 1 demonstrates that the most significant disparity in dose before and after swallowing was observed at energy levels of 60 and 75 keV, specifically for depths shallower than 2 cm. Likewise, for other energy settings, the highest percentage difference was noted for depths equal to or less than 2 cm. Considering that much of the thyroid is located at this shallow depth, reducing the dose through proper timing of swallowing during imaging could be impactful. Instructing patients to avoid swallowing or moving their throat during the 15-second exposure, and imaging during deep exhalation, may effectively minimize radiation delivered to the thyroid. This is because the movement of the thyroid gland to a more shallow and sensitive location can be prevented. Appropriate patient education focused on not swallowing saliva during imaging and instructing patients to remain still with a deep exhalation during exposure has the potential to meaningfully decrease thyroid exposure during panoramic radiography. With proper technique and patient cooperation, radiation doses to the thyroid could be significantly reduced.

To put it differently, in order to explore fluctuations in the absorbed radiation dose received by the thyroid gland during OPG while swallowing, we adopted a novel approach to radiation protection. Our study aimed to investigate potential variations in dose exposure and develop strategies to mitigate any adverse effects on the thyroid gland. The goal was to investigate potential changes in radiation exposure to the thyroid gland specifically during OPG when the patient swallows. By analyzing the absorbed radiation dose in this area, we gained valuable insights to improve radiation safety measures and optimize patient protection. The study aimed to propose innovative techniques for measuring and evaluating variations in the absorbed dose in the thyroid during OPG examinations, focusing on the specific scenario of swallowing. This research initiative aims to contribute to developing strategies that minimize radiation risks and enhance radiation protection protocols in OPG procedures.

Conclusion

The findings of this study validate that swallowing during panoramic radiography increases the absorbed radiation dose to the thyroid gland. While the increase in dose may be small in magnitude, it remains meaningful. Additionally, given the thyroid gland's high radiosensitivity, even modest increases in absorbed radiation can potentially cause significant harm.

Authors' Contribution

H. Vafapour conceived the idea. The introduction of the paper was written by H. Vafapour. The method implementation was carried out by Z. Salehi. Results and Analysis were carried out by Z. Salehi and H. Vafapour. The research work was proofread and supervised by H. Vafapour and Z. Salehi. All the authors read, modified, and approved the final version of the manuscript. All Authors read and approved the manuscript.

Ethical Approval

This study was part of a research project registered with the ethics code of IR.YUMS.REC.1399.0335.

Conflict of Interest

None

References

1. Laishram A, Thongam K, editors. Detection and classification of dental pathologies using faster-RCNN in orthopantomogram radiography image. 7th international conference on signal processing and integrated networks (SPIN); Noida, India: IEEE; 2020. p. 423-8.
2. ALHumaid J, Buholayka M, Thapasum A, Alhareky M, Abdelsalam M, Bughsan A. Investigating prevalence of dental anomalies in Eastern Province of Saudi Arabia through digital orthopantomogram. *Saudi J Biol Sci.* 2021;**28**(5):2900-6. doi: 10.1016/j.sjbs.2021.02.023. PubMed PMID: 34025167. PubMed PMCID: PMC8117041.
3. National Radiological Protection Board. National Radiological Protection Board Account 2004-2005. Corporate report; London: The Stationery Office; 2005. Available from: https://assets.publishing.service.gov.uk/media/5a7586e240f0b6397f35f1cb/0386.pdf.
4. Williams JR, Montgomery A. Measurement of dose in panoramic dental radiology. *Br J Radiol.* 2000;**73**(873):1002-6. doi: 10.1259/bjr.73.873.11064656. PubMed PMID: 11064656.
5. Alterio D, Jereczek-Fossa BA, Franchi B, D'Onofrio A, Piazzi V, Rondi E, et al. Thyroid disorders in patients treated with radiotherapy for head-and-neck cancer: a retrospective analysis of seventy-three patients. *Int J Radiat Oncol Biol Phys.* 2007;**67**(1):144-50. doi: 10.1016/j.ijrobp.2006.08.051. PubMed PMID: 17084554.
6. Chen J, You H, Li K. A review of thyroid gland segmentation and thyroid nodule segmentation methods for medical ultrasound images. *Comput Methods Programs Biomed.* 2020;**185**:105329. doi: 10.1016/j.cmpb.2020.105329. PubMed PMID: 31955006.
7. Khan YS, Farhana A. Histology, Thyroid Gland. In: StatPearls [Internet]. Treasure Island (FL): StatPearls Publishing; 2022.
8. Barbieri A, Prasad ML, Gilani SM. Thyroid tissue outside the thyroid gland: Differential diagnosis and associated diagnostic challenges. *Ann Diagn Pathol.* 2020;**48**:151584. doi: 10.1016/j.anndiagpath.2020.151584. PubMed PMID: 32871503.
9. Braverman LE, Cooper D. Werner & Ingbar's the thyroid: a fundamental and clinical text. Lippincott Williams & Wilkins; 2012.
10. Zhou H, Keall PJ, Graves EE. A bone composition model for Monte Carlo x-ray transport simulations. *Med Phys.* 2009;**36**(3):1008-18. doi: 10.1118/1.3077129. PubMed PMID: 19378761.
11. Morrison GD. Catalogue of Diagnostic X-ray Spectra and Other Data (IPEM Report 78), £20 , K. Cranley, B.J. Gilmore, G.W.A. Fogarty, L. Desponds (Eds.), The Institution of Physics and Engineering in Medicine and Biology (1997), ISBN: 090418188X. *Radiography.* 1998;**4**(3):228-9. doi: 10.1016/S1078-8174(98)80053-9.
12. Kinhikar RA, Tambe CM, Patil K, Mandavkar M, Deshpande DD, Gujjalanavar R, et al. Estimation of dose enhancement to soft tissue due to backscatter radiation near metal interfaces during head and neck radiothearpy - A phantom dosimetric study with radiochromic film. *J Med Phys.* 2014;**39**(1):40-3. doi: 10.4103/0971-6203.125501. PubMed PMID: 24600171. PubMed PMCID: PMC3931227.
13. Jamal NHM, Sayed IS, Syed WS. Estimation of organ absorbed dose in pediatric chest X-ray ex-

amination: A phantom study. *Radiation Physics and Chemistry.* 2020;**166**:108472. doi: 10.1016/j.radphyschem.2019.108472.

14. Rosengren B, Wulff L, Carlsson E, Carlsson J, Montelius A, Russell K, Grusell E. Backscatter radiation at tissue-titanium interfaces. Analyses of biological effects from 60Co and protons. *Acta Oncol.* 1991;**30**(7):859-66. doi: 10.3109/02841869109091835. PubMed PMID: 1662525.
15. Wong JW, Sharpe MB, Jaffray DA, Kini VR, Robertson JM, Stromberg JS, Martinez AA. The use of active breathing control (ABC) to reduce margin for breathing motion. *Int J Radiat Oncol Biol Phys.* 1999;**44**(4):911-9. doi: 10.1016/s0360-3016(99)00056-5. PubMed PMID: 10386650.